



www.ericjournal.ait.ac.th

# An Efficient Regression Prediction Model for Daily Solar Power Generation of Microgrid based on the Collaborative Optimization of Dual-Module GA-BP

Weimin Wu<sup>\*, ^</sup>, Zhaoqin Liu<sup>^ 1</sup>, Yun Wu<sup>#</sup>, Wanjun Yan<sup>\*</sup>, Xiufan Yang<sup>\*</sup>, and Dianxi Zhang<sup>\*</sup>

## ARTICLE INFO

### Article history:

Received 03 September 2025

Received in revised form

25 November 2026

Accepted 12 January 2026

### Keywords:

Daily power generation

prediction

Distributed solar micro-grid

Dual-module dynamic

switching

GA-BP collaborative

optimization

Nonlinear regression

modeling

## ABSTRACT

Combined the backpropagation (BP) neural network with the genetic algorithm (GA), an efficient dual-module regression prediction model is presented for power generation prediction in distributed solar intelligent microgrids. Two years of operation data were collected from a local microgrid system with eight environmental factors as input data. The input data is selected as input of the module, and the cumulative daily power generated by monocrystalline silicon module is used for prediction. The structural framework of the module adopts the dynamic mechanism of switching models. In normal mode, the shallow module (a single-hidden-layer BP network with the GA optimized) is adopted for rapid inference within 0.5 s, and the root mean square error (RMSE) is 62.02W. In more intricate or variable situations, the subsystem activates a deep module (a dual-hidden-layer network trained on 150 generations of GA), and the results are highly accurate and decrease the RMSE to 20.93W and increase the coefficient of determination (R<sup>2</sup>) to 0.943. The onset time of light intensity precedes that of ambient temperature by one to two hours, resulting in an average relative prediction error within 3%. The efficiency of power scheduling can reach more than 30% by adjusting power allocation and optimize energy curtailment. The proposed framework can obtain effective balance between computation and forecasting precision, providing a realistic and reliable solution for on-line energy management in microgrid applications.

## 1. INTRODUCTION

Distributed solar smart microgrids represent a promising technology with broad development prospects. Its performance is crucial for enhancing system stability and economy [1]. Key obstacles such as intermittent power supply and the need for multi-source coordination require technological innovations in intelligent regulation and control [2], energy storage optimization [3] and energy management [4], thereby fully leveraging its potential in power supply for remote areas and low-carbon transformation. There has been rapid growth in addressing the challenges of distributed solar microgrids, such as intelligent control, energy storage optimization, power management, intermittent supply, and multi-source coordination. Arkhangelski *et al.* [5]

discussed the importance of day-ahead optimal power flow for efficient energy management of urban microgrids. Zhang *et al.* [6] proposed a multi-energy complementary linkage technology for economic evaluation to optimize the development and utilization of wind and solar energy. Elgammal *et al.* [7] focused on creating an optimal energy management strategy for a DC linked hydro-PV-wind renewable energy system to minimize grid imported energy costs. Kumar *et al.* [8] explored energy management of renewable energy-based microgrid systems with hybrid energy storage systems for various operation modes. Barua *et al.* [9] investigated heuristic and optimization energy management algorithms to minimize residential electricity costs, emphasizing the importance of optimal control for effective energy delivery. Mohan *et al.* [10] presented an optimized power flow management system based on Harris Hawks of an islanded DC microgrid with distributed generation sources. Siddaraj *et al.* [11] proposed a hybrid MPPT method based on PSO-ANFIS for coordinated power management of microgrids with solar PV plants and battery energy storage systems, so as to improve PV potential extraction. Elalfy *et al.* [12] proposed a frequency regulation method based on the antlion optimization approach to electric vehicle involved in microgrid with the objective of optimizing charging and discharging power. Lv *et al.* [13] proposed multiple stages constraint-handling multi-objective optimization approach to resilient microgrid energy

DOI: <https://doi.org/10.64289/iej.26.0103.7975642>

<sup>\*</sup>School of Electronic and Information Engineering, Anshun University, Anshun, 561000, China.

<sup>^</sup>School of Aeronautical Mechanical and Electrical Engineering, Chongqing Aerospace Polytechnic, Chongqing, 400021, China.

<sup>#</sup>Yinchuan University of Science and Technology, Yinchuan, 750001, China.

<sup>1</sup>Corresponding author:

Tel: +86 023-67613088

Email: [zqin\\_liu\\_cap@163.com](mailto:zqin_liu_cap@163.com)

management. The performance was shown to be superior when compared to other optimization algorithms. Agupugo *et al.* [14] presented the least achievements and techniques for microgrid operation optimization using renewable energy, based on a robust advanced methodology. Optimization techniques including MPC, MILP, and heuristics algorithms in real time energy production and distribution re-allocation. Ersöz *et al.* [15] showed that the XGBoost, CatBoost, AdaBoost, and LightGBM boosting methods belong to ensemble learning methodologies, and are highly efficient for renewable energy prediction. This shows ensemble approaches have a bright prospect in the output forecasting abilities. Alagappan *et al.* [16] proposed a BagANN ensemble and further optimized it by applying the Grey Wolf Optimization Algorithm (GWO). It aims to adjust system hyperparameter and strengthen the predictability of output, as well as how much the optimization is essential to improve ensemble model for solar power forecasting. In 24-hour photovoltaic power forecasting, Al-Dahidi *et al.* [17] used Genetic Algorithm, Ant colony optimization (ACO) algorithm and Bat algorithm to optimize ensemble size and rule base design. They found that the Bat algorithm could enhance the forecasting by utilizing their tactics in proper and systematic manner for rule base creation. Dahidi *et al.* [18] proposed a Bayesian information-based ensemble model, which focuses on rule-based prediction models and Bagging prediction models. The average prediction accuracy was improved to 97.32%, and an ensemble learning strategy was introduced to enhance prediction and forecasting using non-stationary strategies. In addition, this strategy was used to add non-stationary data into a large dataset obtained using sequential sampling [19]. This approach can incorporate more non-stationary data into time-series prediction. Furthermore, a hybrid meta-heuristic ensemble approach was introduced to compute the optimal system parameters for PM prediction [20]. The cost function value of PM integrated prediction models has been effectively reduced by implementing mixed meta heuristic methods, with the cost of these models being less than 20%. Al-Ghussain *et al.* [21] proposed a method of mapping an Inland Dew Point (IDP) into a Computed Cloudiness (CC) to calculate a sun position (SP) for the sun path. This mapping utilized the EC-MT and an optimization strategy, Genetic Algorithm (GA) to map the solar path values to the sky model. Simulation shows that this mapping results in an average error of 7% for the east-west azimuth angle in 24-hour sunshine. The technical and economic feasibility of photovoltaic (PV) charging stations in developing countries under summer and winter has been tested and analyzed on a pilot basis in Jordan. An optimizer was implemented for a battery-charging station to find the highest profit, providing useful feasibility information for an investor planning to install a green charging network. The PV-Zn-Br achieved the highest annual profit reaching 7535 USD. Al-Dahidi *et al.* [22] introduced a data-driven model with feature transformation and extraction, considering new features extracted from the physical principle of photovoltaic systems to improve the

predictive accuracy. The accuracy of this model can be improved by 21% and 64%, respectively compared to traditional feature sets and PCA.

For optimizing the control strategies, real-time and quick analysis of a large quantity data generated in intelligent microgrid is needed, such as meteorological data, equipment status data and power data to monitor and control the operating status of microgrid system, thus further improving the reliability and stability of supply in distributed solar intelligent microgrid system. Nevertheless, for the data of the distributed solar intelligent microgrid, we will face numerous problems like low processing speed, low modeling efficiency, and inaccurate performance prediction, with traditional data processing and modeling methods encountering a large scale, complex and real-time changing data and being difficult to satisfy the rapid decision-making and exact control requirements of microgrid. Hence, fast modeling and performance prediction of distributed solar intelligent microgrids will be needed for such research. This study puts forward the data regression rapid prediction model based on BP (back propagation) neural network optimized by GA, so as to realize the rapid construction of high-dimensional complicated physical data of distributed solar intelligent microgrid system, accurately forecast the related key performance indicators, help operation maintenance personnel to formulate reasonable operation and maintenance plans, so as to effectively enhance the efficiency and reliability of operation of microgrids, and reducing operating costs and risks.

The organizational structure is: Section 2 gives a principle-based explanation of BP neural network algorithm and genetic algorithm, as well as a comparative analysis of their advantages and disadvantages; Section 3 proposes a dual-module high-efficiency regression prediction model based on the collaborative optimization of BP-GA; Section 4 conducts an analysis and discussion on the regression prediction results. Finally, critical conclusions and insightful closing discussions are presented.

## 2. ALGORITHM FOUNDATION

### 2.1 BP Neural Network Algorithm

The mechanism of the Back Propagation (BP) neural network (*i.e.*, a feedforward neural network with backpropagation) is to iteratively adjust the network weights and biases to make the difference of outputting between the network and the expected target values minimized.

#### 2.1.1 Forward propagation

In forward propagation step the input signals flows through each layer of the network to reach output layer.

- 1) From input layer to hidden layer

Assume there is an input layer with an input vector  $X = [x_1, x_2, \dots, x_n]$ , and a hidden layer with  $m$  neurons. The weight matrix is denoted as  $W^{(1)}$  and the bias vector as  $b^{(1)}$ . The input  $a_j^{(1)}$  and output  $h_j^{(1)}$  of the  $j$ -th neuron in the hidden layer are calculated as follows:

$$a_j^{(1)} = \sum_{i=1}^n W_{ji}^{(1)} x_i + b_j^{(1)} \quad (1)$$

$$h_j^{(1)} = f(a_j^{(1)}) \quad (2)$$

where  $f(\cdot)$  is the activation function, with commonly used functions of Sigmoid, Tanh, and ReLU.

2). From hidden layer to output layer

Assume the output layer has  $k$  neurons, with a weight matrix  $W^{(2)}$  and bias vector  $b^{(2)}$ . The input  $a_1^{(2)}$  and output  $y_1$  of the  $l$ -th neuron in the output layer are calculated as follows:

$$a_1^{(2)} = \sum_{j=1}^m W_{lj}^{(2)} h_j^{(1)} + b_l^{(2)} \quad (3)$$

$$y_1 = f(a_1^{(2)}) \quad (4)$$

### 2.1.2 Loss function

Loss function the loss function quantifies how much the network output deviates from the target value. The mean squared error (MSE) loss is a frequently used loss function:

$$L = \frac{1}{2} \sum_{i=1}^k (y_i - t_i)^2 \quad (5)$$

where  $t_i$  is the target value.

### 2.1.3 Back propagation

Back propagation back propagates errors and updates weights and biases of the model by solving gradient descent algorithm to ensure minimization of loss function.

1) Gradients at the output layer

As for the partial derivative of the input of the loss function, we take the partial derivative of Equation (17) with respect to the input as follows.

$$\delta_1^{(2)} = \frac{\partial L}{\partial a_1^{(2)}} = (y_1 - t_1) f'(a_1^{(2)}) \quad (6)$$

2). From hidden layer to output layer

The weight and bias are updated using the gradient decent rule as follows:

$$W_{ji}^{(1)} \leftarrow W_{ji}^{(1)} - \eta \delta_j^{(1)} x_i \quad (7)$$

$$b_j^{(1)} \leftarrow b_j^{(1)} - \eta \delta_j^{(1)} \quad (8)$$

$$W_{lj}^{(2)} \leftarrow W_{lj}^{(2)} - \eta \delta_l^{(2)} h_j^{(1)} \quad (9)$$

$$b_l^{(2)} \leftarrow b_l^{(2)} - \eta \delta_l^{(2)} \quad (10)$$

where  $\eta$  is the learning rate.

The logical architecture of this BP neural network algorithm is shown in Figure 1.

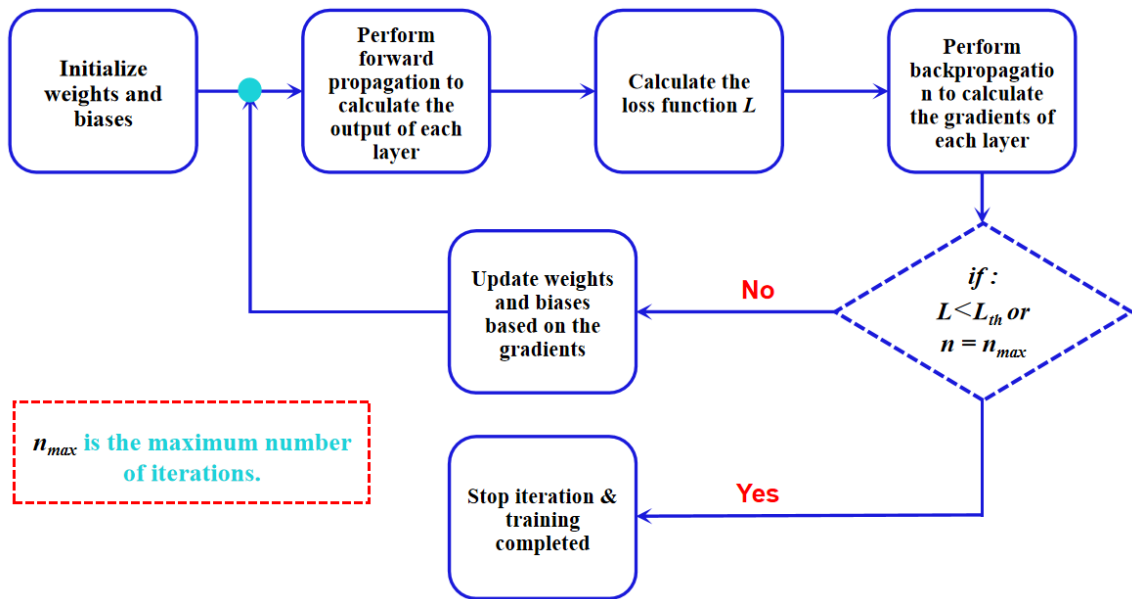


Fig. 1. The logical flow of the BP neural network algorithm.

## 2.2 Genetic Algorithm

Genetic algorithms (GA) are nature-inspired evolutionary optimization algorithms which use processes like natural selection, crossover, mutation to explore an optimization space for an optimal solution.

### 2.2.1 Individual representation (encoding)

For distributed solar microgrids, continuous variables (such as power generation capacity, energy storage capacity, load demand) need to be optimized. Real

number encoding directly represents the real physical quantities, avoiding the quantization errors of binary encoding and improving the optimization accuracy. At the same time, it supports arithmetic crossover and Gaussian mutation, which can finely adjust parameters in the continuous space and adapt to real-time fluctuations of microgrids.

In this case, real number encoding is introduced. Each individual (candidate solution) is a vector of real numbers:

$$x = [x_1, x_2, \dots, x_n], x_i \in [a_i, b_i] \quad (11)$$

where  $a_i$  and  $b_i$  indicate the domain bounds of the  $i$ -th parameter.

### 2.2.2 Population initialization

$N$  individuals are generated randomly within the domain:

$$x_i^{(j)} = a_i + \text{rand}(0,1) \times (b_i - a_i) \quad (12)$$

where  $x_i^{(j)}$  is the  $i$ -th parameter of the  $j$ -th individual, and the  $\text{rand}(0,1)$  is the uniform random number in  $[0,1]$ .

### 2.2.3 Fitness function

Solution quality is sometimes measured by a fitness function.  $F(x) = \frac{1}{1+f(x)}$  or  $F(x) = -f(x)$  is for minimization, and  $F(x) = f(x)$  for maximization. Conventional logic is that the higher the fitness value, the better the individual. Meanwhile, the fitness value can be scaled linearly or exponentially to avoid premature convergence.

### 2.2.4 Selection operators

Superior individuals based on fitness are selected as the parent generation. The commonly used methods include roulette wheel selection and tournament selection. Here, roulette wheel selection is used to balance "exploitation" (utilizing high fitness individuals) and "exploration" (maintaining the diversity of low fitness individuals) through a probability allocation mechanism. The probability of selection is as follows:

$$P(x_i) = \frac{F(x_i)}{\sum_{j=1}^N F(x_j)} \quad (13)$$

The cumulative probability is as follows:

$$Q(x_i) = \sum_{k=1}^i P(x_k) \quad (14)$$

where a random number  $r \in [0,1]$  is generated and the individuals that satisfy  $Q(x_{i-1}) \leq r < Q(x_i)$  are selected.

### 2.2.5 Crossover operators

Here, arithmetic crossover is adopted to generate offspring through weighted averaging, ensuring that the corresponding continuous variables of the solar micro-grid are adjusted smoothly during optimization, avoiding sudden changes and maintaining the physical feasibility and stability of the micro-grid. Two parents are blended using a weight  $\alpha \in [0,1]$ , and the corresponding calculation formula is as follows:

$$y_1 = \alpha x_A + (1 - \alpha)x_B; y_2 = (1 - \alpha)x_A + \alpha x_B \quad (15)$$

### 2.2.6 Mutation

The Gaussian mutation of GA can adapt to the uncertain data of the distributed solar energy by adding normal distribution perturbation, and its adjustment of the variation characteristic can improve the proportion of local search and global search, optimizing the ability and

accuracy of robustness of the algorithm under the uncertain environment. Real-number mutation adds small perturbation to ensure diversity.

$$x_i' = x_i + \delta, \quad \delta \sim N(0, \sigma) \quad (16)$$

where  $\delta$  follows a Gaussian distribution.

### 2.2.7 Generate a new generation of population

With the implementation of the Elite retention strategy, the best individuals of parent generation are directly retained and strong ones of the parent generation are not lost because of the implementation of genetic operations and the population diversity is retained to some degree so that the convergence efficiency of the algorithm as well as the population diversity are well balanced; this optimizes and stabilizes the fluctuation of solar energy data and the model optimization of the microgrid.

### 2.2.8 Termination condition

It is terminated when any of the following conditions is met. It includes reaching the maximum number of iterations  $T_{\max}$ , convergence of fitness values (such as no change in the optimal fitness value for consecutive generations), and finding satisfactory solutions such as  $F(x) \geq F_{\text{target}}$ .

The logical architecture of the genetic algorithm optimization is shown in Figure 2.

## 2.3 Advantages and Disadvantages of BP and GA

BP neural network has the main characteristic of the highly nonlinear modeling capacity. Combined with the backpropagation, it learns the hidden patterns in data by modifying the weights of each neuron. It can learn the pattern of complex data and perform extremely well for image recognition, time series prediction, etc. The shortcomings is apparent as well: it needs to find suitable initial parameters by using gradient descent method, but the training tends to be trapped in local optimization. The training process strongly depends on abundant high quality labeled training data and data noise, or lack of data directly impacts model generalization. In addition, when training deep networks, it is easy to encounter the problem of gradient vanishing or explosion, and the efficiency of training is low. GA is based on the theory of biological evolution and realized global search through population selection, crossover and mutation operations. It is especially fit for solving high-dimensional complex problem including multi-peak optimization or non-convex function. Its merits are no need the objective function's differential, ignoring the first value parameters, effectively eliminating local optima. It is good at discrete optimization (such as path planning) and adapt to dynamic environments. The computation of GA is high. Many resources are occupied by population iterations and the convergence speed in the later phase is slow. Algorithm parameters (e.g. crossover rate and mutation rate) need to be set empirically, and wrong settings will cause premature convergence or reduce the searching efficiency.

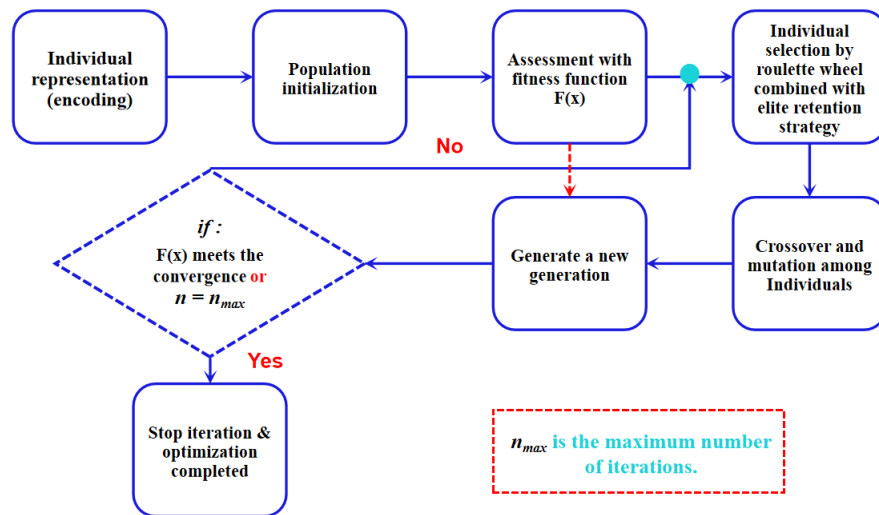


Fig. 2. The logical flow of the genetic algorithm..

In combination with GA, BP neural network can build a “global-local” two-level optimization framework to fully play the complementary strengths. In terms of parameter optimization, the global search is carried out by genetic algorithm as the initial weights and thresholds of BP network, so as to avoid gradient descending becoming stuck at the local minimum. At the same time, it optimizes the hyperparameter such as the learning rate and the momentum factor. Thus, effectively improves the training efficiency. For instance, on the basis of the genetic algorithm screening possible high interest rate, low-risk investment portfolio intervals in the finance field, the BP network can be used to model the nonlinear fluctuation characteristics of the market. On structural design level, genetic algorithm can automatically search for the best neural network’s topology structure (such as the number of hidden layer nodes, type of activation function), which can reduce the manual trial and error cost and improve the model’s robustness. On dynamic adaptation and real-time optimization level, the convergence has high strategic value. GA can periodically optimize the parameter setting of BP network to follow data distribution drift (for example monitoring the change in industrial equipment). BP network refines the candidate solutions, which are yielded by GA by rapid backpropagation, realizing the mechanism of “rough screening and refine refinement” collaboratively. These kinds of hybrid strategies have been widely used in the aerospace (e.g., aircraft trajectory optimization), intelligent manufacturing (e.g., composite material fatigue lifetime prediction) and others. Their fundamental meaning is to co-evolve global exploration and local exploitation abilities, and take computation cost and model precision into account, offering the theoretical and technical basis for the effective modeling and real-time decision making of complicated systems. It is noted that the overall path of the two algorithms above can also serve as an effective theoretical reference of effective integration of highly turbulent renewable energy sources, such as the case of the regression prediction problem for distributed solar intelligent microgrid systems.

### 3. A HIGH-EFFICIENCY REGRESSION PREDICTION MODEL WITH BP-GA SYNERGISTIC OPTIMIZATION

This architecture addresses the need for real-time scheduling speed in intelligent microgrids by introducing a combined-module dynamic switching model through the GA and BP-neural network, as shown in Figure 3. In this study, two years of historical operational data information from a local distributed solar microgrid system are used as the experimental data. The database includes eight environmental parameters: humidity, temperature, noise, PM2.5, PM10, TSP, pressure, and irradiance. Data was collected hourly, resulting in over 17,000 valid samples that capture seasonal and weather-related variations.

A shallow neural network with a light weight is taken as the upper module (GA-BP-Shallow Layer). GA is used to update the weights and threshold of a one-hidden-layer BP neural network. 100 individuals are randomly initialized in a real valued coding schema of this network. Arithmetic crossover (crossover probability: 0.8) and non-uniform mutation (mutation probability: 0.05) are used to create new individuals, avoiding the strong dependency of traditional BP networks to initial parameters. The elite preservation and roulette wheel selection mechanism are adopted for selecting. The number of generational limit is 150 generations and the fitness limit is  $1 \times 10^{-6}$ . It needs to be terminated when the prediction accuracy reaches the established criterion. The output results are immediately print to achieve a response speed of less than 0.5 s, meeting the needs of high frequency scheduling in microgrids.

If the upper module cannot converge when there is a strong nonlinear dynamic of a sudden cloud cover change, the system will automatically invoke the lower module (GA-BP-Deep Layer) composed of a double hidden layer architecture to support its feature representation capability of additional deep module of two sigmoid activation functions (logsig). The number of nodes in the hidden layers is shown in Figure 3. The GA generations are increased to 150 to optimize a more

involved parameter space. Even though the computation time increases by more than 40%, there is still an 18% - 22% improvement in prediction under more complex conditions. For dataset preprocessing, we randomly

select the training and testing sets (with sizes of 70% and 30%, respectively) to ensure that each of them has the same probability representation (without overfitting).

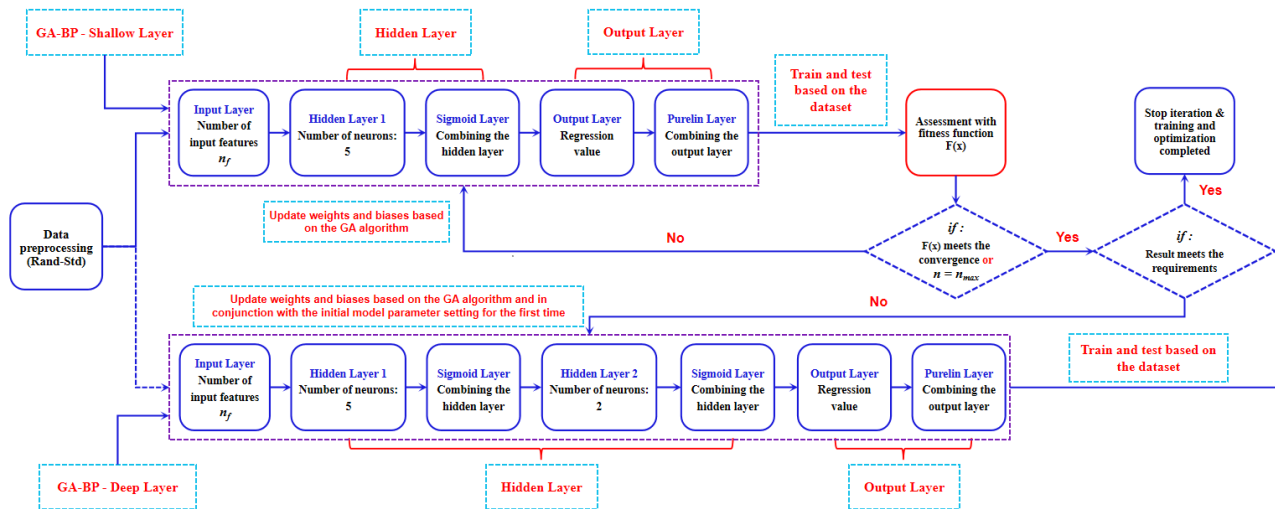


Fig. 3. The logical architecture of the efficient regression prediction model based on BP-GA.

To conduct benchmark testing, a traditional model (*i.e.* a separate BP neural network and support vector machine (SVM) regression model) was deployed as a baseline to rigorously validate the effectiveness of the proposed dual module framework. The scheme of training/testing is consistent (70% and 30% train and test) through random sample shuffling to ensure statistics. Based on the dynamically module selection, compared with the single model, the integrated framework reduces the overall computation more than 30% while keeping the prediction error of  $\leq 3\%$ . The synergy of these methodological innovations ensures transparency, reproducibility and robustness, laying a solid foundation for practical implementation of microgrid energy management systems. The data is from the real-life dataset recorded by the intelligent microgrid operation system of Yinchuan University of Science and Technology in Ningxia Hui Autonomous Region. It is one of the main infrastructure constructions for the campus electricity supply system, campus green energy system, intelligent microgrid and advanced information technology in smart electricity grids.

## 4. DISCUSSION ON THE CALCULATION RESULTS

### 4.1 Sample Data Analysis

The data of distributed solar intelligent microgrid system has a series of variation characteristics. The eight feature parameters (humidity, temperature, noise, PM2.5, PM10, TSP suspended particulate matter, atmospheric pressure, and light intensity) optimized by genetic algorithm for BP neural network are used to predict the cumulative daily power generation of monocrystalline silicon. The target value of the cumulative daily power generation of monocrystalline silicon has significant periodic-like fluctuation characteristics. Light intensity has a positive correlation with it. However, due to different unit

dimensions of the features and the influence of other features and microgrid regulation, there are significant nonlinear characteristics between light intensity and the target value, as shown in Figure 4(a).

The visualization effect in Figure 4(b) was purposely adjusted so as to draw attention to those factors that contribute the most to environmental factors in single-crystal silicon power generation process. By the process of selectively bolding curves and adjusting visualization techniques, the three principal features Feature 8 (light intensity), Feature 2 (temperature), and Feature 7 (atmospheric pressure) are highlighted. These are features, that physically affect the PV performance the most: light intensity directly affects the amount of photon used to make electricity; temperature is proportional to the semiconductor bandgap properties and the panels' overall efficiency (typically inversely to the panels' output, once they exceed the ranges with maximum efficiency); and atmospheric pressure is correlated with the air density and therefore convective cooling of the panels. We can easily see from this figure of visual optimization how these major factors govern the multi-peak power generation curve of each day and their coherent fluctuation constitutes the major characteristic of multi-peak power generating curves, which is illustrated in Figure 4(a), especially the bold curves exhibit the phase-differences between parameters in time dimension. For instance, the maximum light intensity around solar noon occurs 1-2 hours earlier than the maximum temperature, and the way these phenomena alter with atmospheric pressure through the weather systems and give a self-consistent effective reference to unveil the complicated physical mechanisms underlying the performance of solar microgrids.

In addition, we should consider that autonomous regulating mechanism of microgrids such as maximum power point tracking algorithm and load balancing

algorithm are more nonlinear terms due to system parameters are be dynamically regulating according to real-time operation condition. Such complex interrelationships result a unique response pattern in which even a weak enhancement of the light intensity

may make power output reducing or an occasionally even more extensive increase, evidencing the pivotal role of the multivariate analysis of the microgrid intelligence, as well as the subsequent more precise nonlinear prediction for power generation regression.

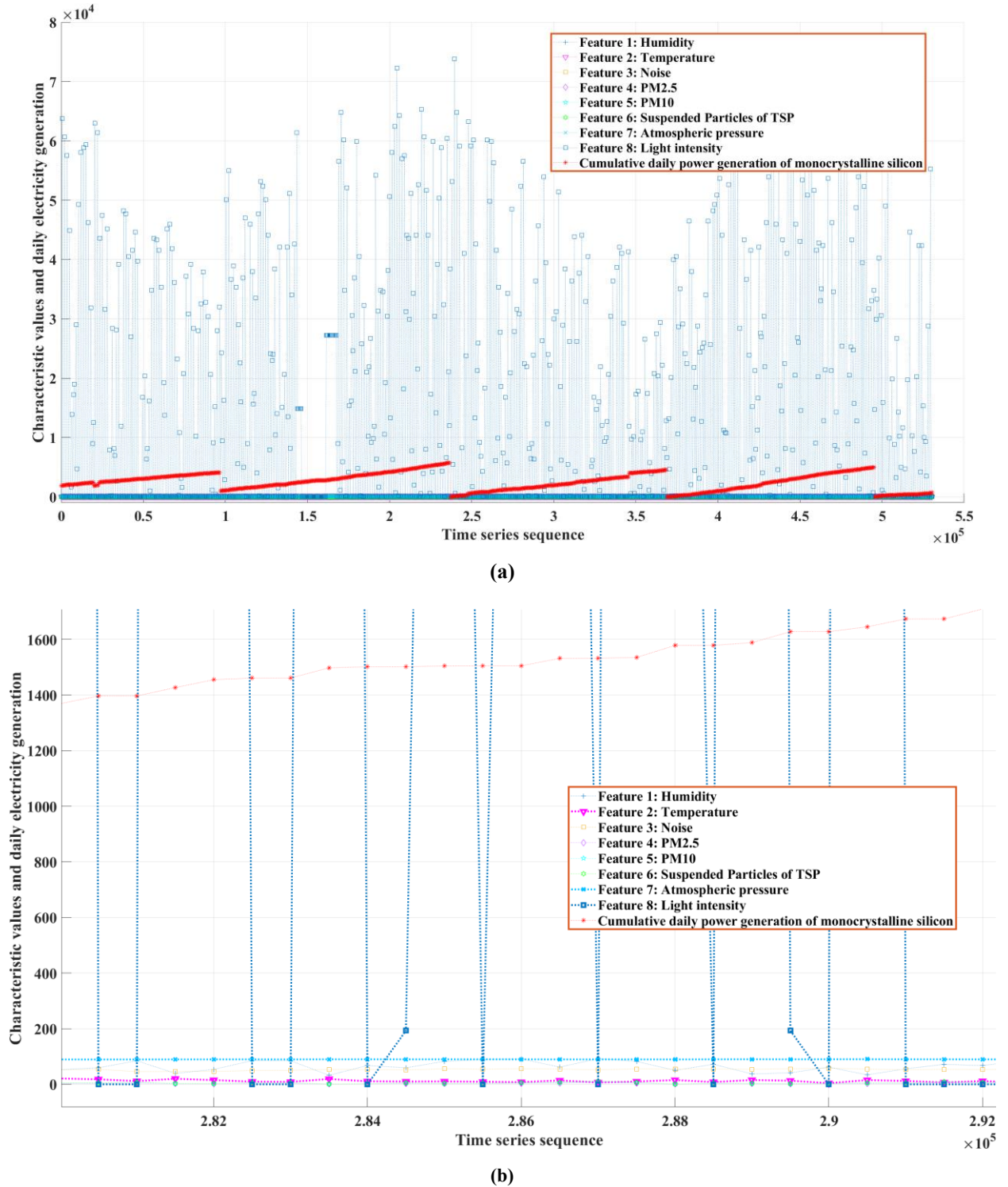


Fig. 4. A series of variation characteristics of data in the distributed solar intelligent microgrid system.

#### 4.2 Comparison of Fitness Value Changes

Considering the multi physics coupling mechanism of monocrystalline silicon power generation, the advantages of GA-BP deep module in distributed solar microgrid data optimization can be explained (Figure 4 (a)). The shallow model (GA-BP-Shallow-Layer) is

limited by the depth of the network and can only capture linear or simple nonlinear relationships between light intensity (Feature 8) and power generation (such as positive correlation trends), and cannot analyze the synergy effect of light intensity-temperature-atmospheric pressure (Features 2/7/8). For example,

when the light intensity reaches its peak at noon, high temperature leads to a decrease in the efficiency of photovoltaic panels (decreased semiconductor carrier mobility). However, changes in atmospheric pressure regulate the heat dissipation efficiency through air density, and the three factors jointly form the multi-peak power generation curve, as shown in Figure 4(a). The deep model (GA-BP-Deep-Layer) can construct a cross-scale feature interaction network through multi-layer nonlinear activation functions and the global search ability of genetic algorithms, accurately quantifying the weight distribution of the main effect of light intensity, the negative feedback effect of temperature, and the indirect regulatory role of atmospheric pressure, thereby achieving better convergence in fitness values (Figure 5 red curve). This ability enables it to be compatible with the time phase differences as shown in Figure 4(b) (For example, the light intensity peak appears 1-2 hours earlier than the temperature peak), effectively avoiding prediction deviations caused by asynchronous parameter fluctuations.

The delay convergence characteristic of the GA-BP-Deep-Layer module (60 generations) is highly compatible with its demand for handling complex physical scenarios. In the single-crystal silicon power generation system, although light intensity is the

dominant factor, its contribution to power generation is dynamically adjusted by temperature and atmospheric pressure (the difference in the curve in Figure 4(b)). The essence of rapid convergence of the shallow model (25 generations) is to sacrifice the resolution accuracy of secondary features and retain only the linear principal components of light intensity, resulting in a high fitness value (the blue curve in Figure 5). In contrast, the deep model extends the genetic generations to systematically explore the following coupling relationships in the solution space: 1) The nonlinear antagonistic effect of light intensity and temperature (high temperature weakens the photon-electric energy conversion efficiency); 2) The regulation of atmospheric pressure on thermodynamic boundary conditions (low-pressure environment reduces convective heat dissipation rate and exacerbates the negative temperature effect); 3) The normalization processing of multi-feature dimensional differences (such as the physical unit span between PM2.5 and light). This enables it to approach the global optimal solution of the multi-peak curve in Figure 4(a). Furthermore, it enhances robustness against meteorological perturbations such as abrupt PM10/TSP increases during sandstorms, providing a highly reliable basis for real-time microgrid scheduling decisions.

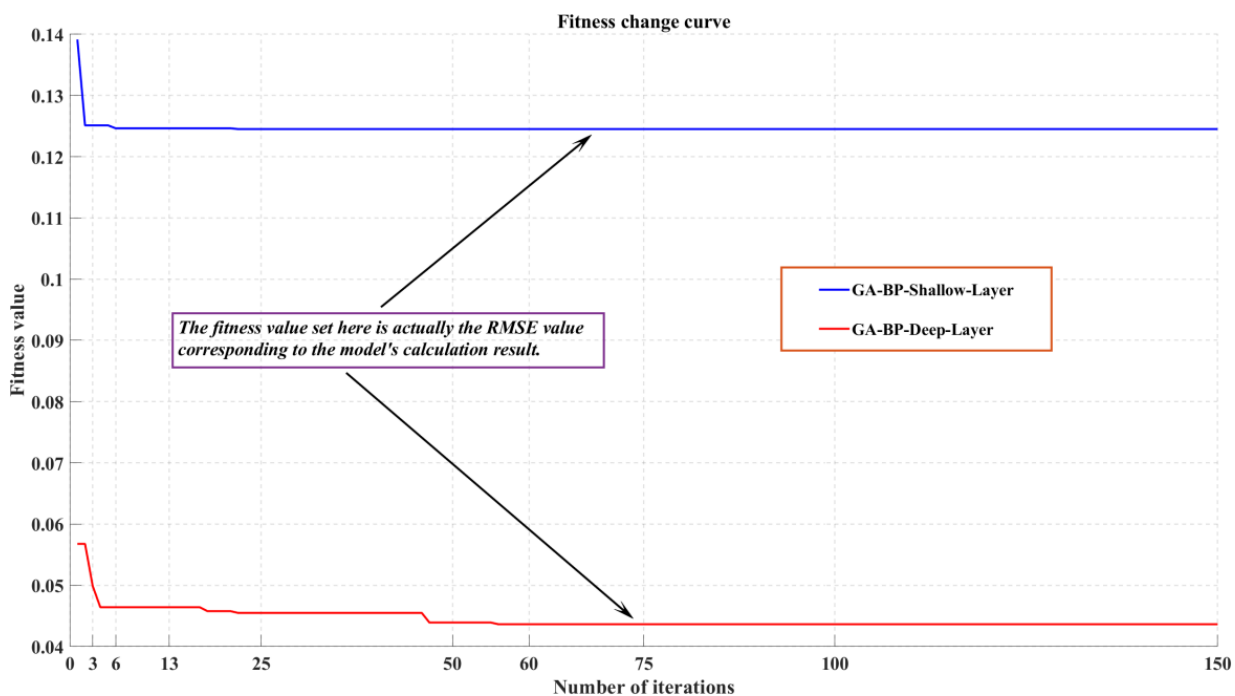
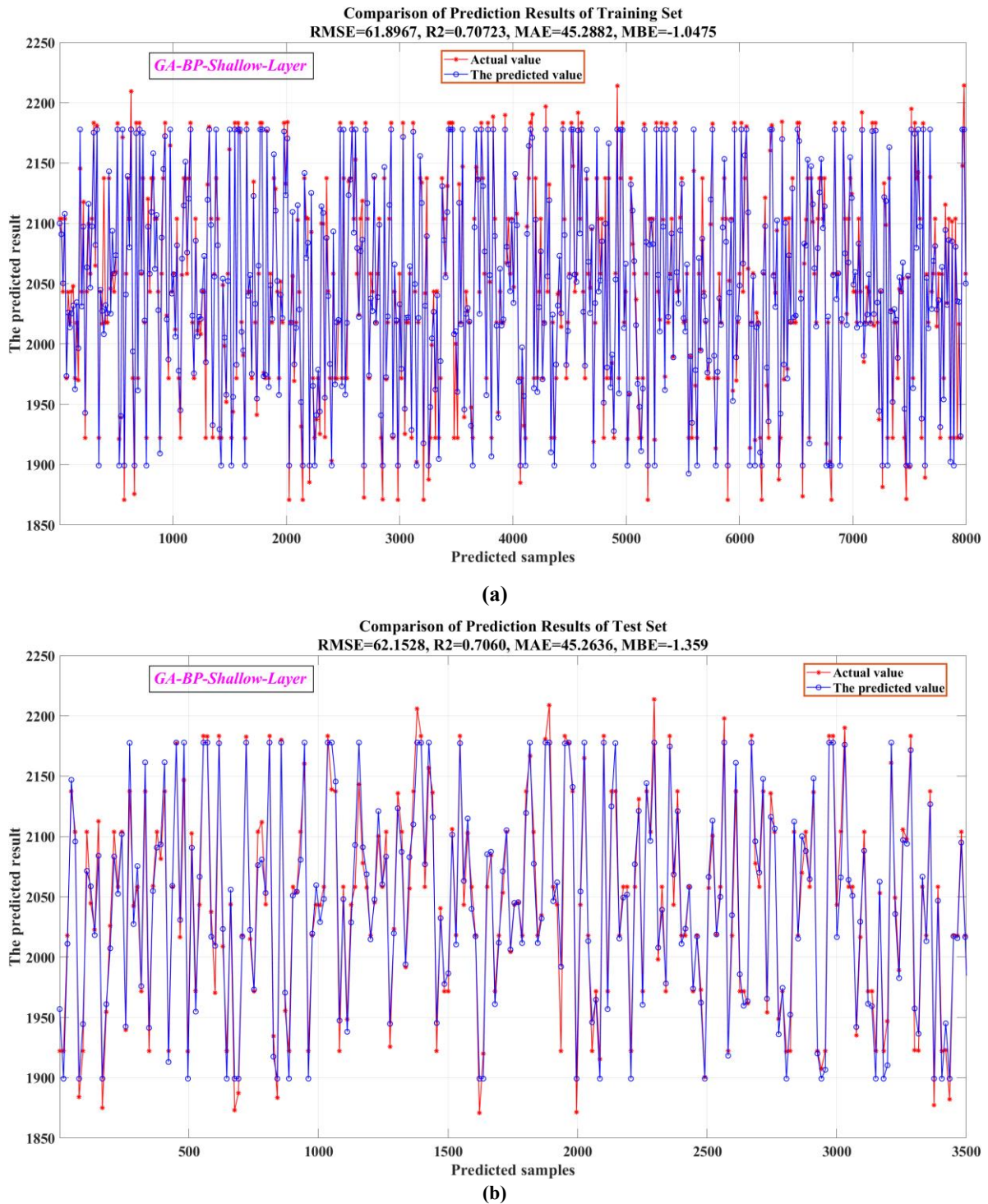


Fig. 5. Comparison of fitness curve variations for GA-BP-Deep-Layer and GA-BP-Shallow-Layer.

### 4.3 Analysis of GA-BP Dual-module Prediction Results

Figure 6(a) shows the computational results of the training set obtained using the GA-BP-Shallow-Layer module. Figure 6(b) shows the corresponding

performance on the test set under the same model configuration. Similarly, Figure 7(a) shows the training set results generated by the GA-BP-Deep-Layer module, and Figure 7(b) shows the respective test set results using the identical architecture.



**Fig. 6. Regression prediction results of the GA-BP-Shallow-Layer module (RMSE unit: W).**

The GA-BP-Shallow-Layer module is based on a single-hidden-layer BP neural network model. It uses GA to improve the initial weight and threshold of the model and realize rapid response: the prediction duration can be realized under 0.5 s. Combined arithmetic crossover with non-uniform mutations strategies, the model can reduce the sensitivity of traditional BP network to initial parameter setting, but shallow structure limits its global approximation. The RMSE and R-squared calculated by the model on the training and testing sets are 62.02 W and  $R^2$ , respectively. It is approximately 0.707, indicating that the model's feature learning ability, especially for complex nonlinear

relationships, is limited. The GA-BP-Deep-Layer module improves feature learning through a double-hidden-layer architecture. Two log-sigmoid functions are used to activate and extend the genetic evolution from 100 to 150 generations to optimize more parameters. Therefore, the RMSE is reduced significantly to 20.93 W and  $R^2$  is increases to 0.943. The calculation time only increased by 40%. Due to the dynamic switching mechanism of the model on the error threshold ( $RMSE \leq 3\%$ ), the overall system efficiency improves by more than 30%. This is particularly evident under complex operating conditions, such as sudden weather changes.

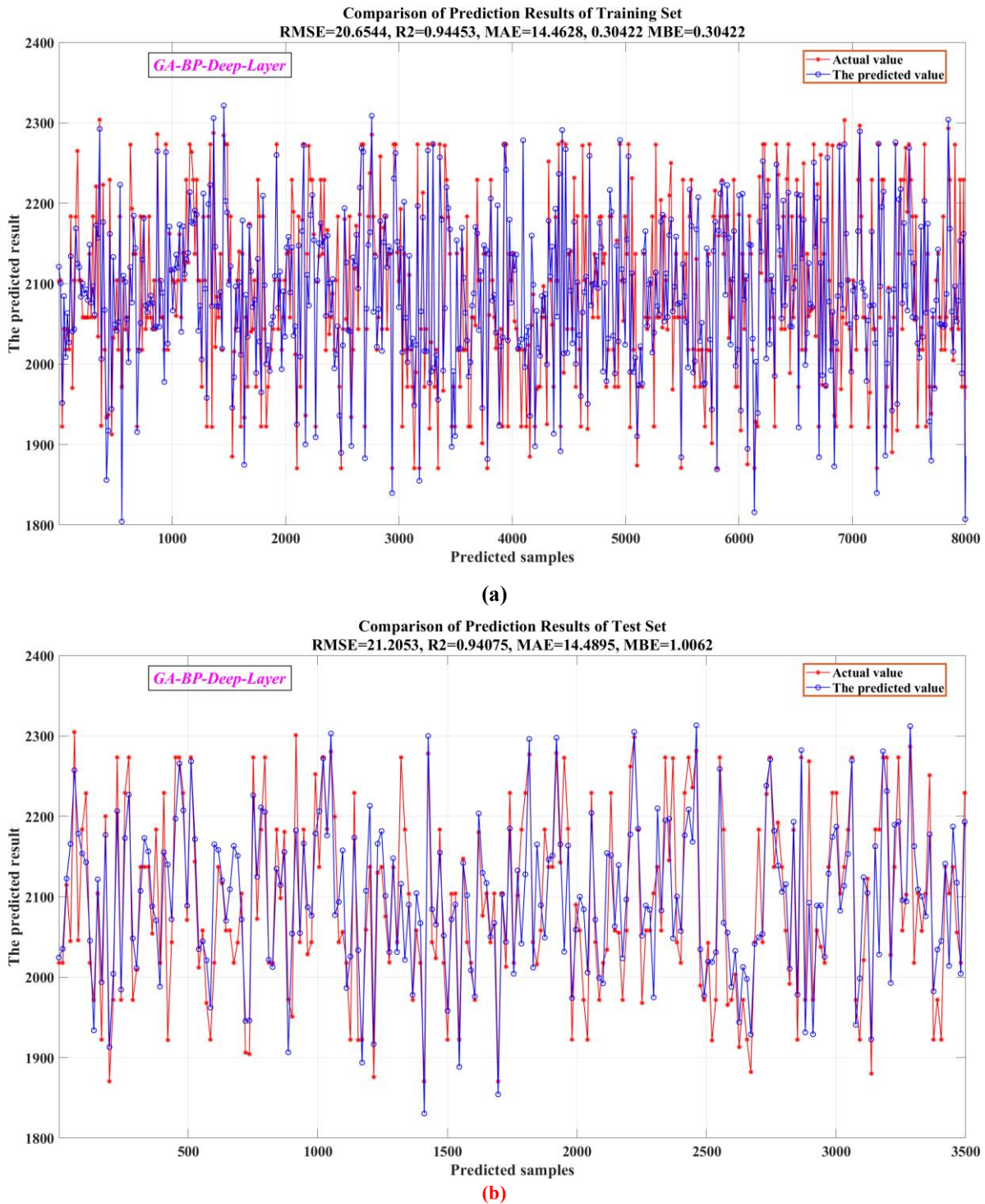


**Fig. 7. Regression prediction results of the GA-BP-Deep-Layer module (RMSE unit: W).**

In error measurement, the shallow module has a lower degree of degradation between training and testing data, with an RMSE difference of only 0.26 W (61.90 W and 62.15 W) and a MAE difference of only 0.02 (45.29 and 45.26). The accuracy is still relatively low, but it has stable generalization ability because a negative MBE of -1.05 to -1.36 W implies systematic bias in underestimation. The deep module has an RMSE of 20.65 W ( $R^2=0.70$ ) and a  $R^2$  score of 0.68 on the test set. We achieve 21.46 W (MSE = 0.945) on the training set and 21.21 W (MSE = 0.941) on the test set, with a fluctuation error of only 2.7%, demonstrating high robustness. MBE changes only 0.30 W (training) to 1.01 W (test), indicating a mild overfitting to the deeper

architectures when modeling a high nonlinearity pattern. Moreover, the deep module further obtains more precise physical interpretation on the key environmental factors including light intensity and temperature (Figure 4(b)) instead of monotonous global compensation from single non-linear component. It can capture the time-phase difference between multi-peak power generation profiles to overcome the shallow model in strong nonlinear field.

Shallow modules can meet the high scheduling frequency requirements such as real-time power dispatch under stable weather conditions. Quick response can match sub-second control and dispatching demand of micro-grid well; otherwise, for environmental parameters change events (such as

nonlinear change of solar irradiance due to variation of cloud-cover), when model failed to converge, system would fall into deep module. The later increases the multi-feature coupled effect modelling ability by adding more hidden layer neurons (see Figure 3) to better reflect the synergistic relationship in the light intensity, temperature and atmospheric pressure of variables. For instance, the multi-peak power generation shape is

shown in Figure 4(a). Through the experimental results, when the operating condition of the microgrid is complicated, the prediction accuracy of the prediction module will increase 18-22%. The calculation delay of the prediction module should also be considered carefully according to the adjustment time window of the microgrid.

Table 1 shows the model configuration.

**Table 1. Model configuration.**

Components	Parameters	Values/Settings
Dataset	Timespan	2 years
	Collection Frequency	Hourly
	Sample Size	>17,000
	Source	Yinchuan University of Science and Technology, Ningxia
GA	Population Size	100
	Encoding	Real-valued
	Crossover Probability	0.8 (Arithmetic)
	Mutation Probability	0.05 (Non-uniform)
	Selection Strategy	Roulette Wheel and Elite Preservation
	Termination Criteria	150 generations or fitness $< 1 \times 10^{-6}$
BP Network	Hidden Layers	Shallow: 1, Deep: 2
	Activation Function	Double Sigmoid (logsig)
	Training Set Ratio	70%
	Test Set Ratio	30%
	Hidden Layer Nodes	As shown in Figure 3
	Training Epochs	150
	Learning Rate	0.01
	Momentum Factor	0.9

This switching dynamic strategy is triggered by "70%" of the training set and random permutation, balancing generalization ability by effectively balancing minimizing overtraining and improving prediction model efficiency.

## 5. CONCLUSION

Combined genetic algorithm (GA) with backpropagation (BP) neural network, we present a dual-module dynamic switching prediction model for distributed solar-driven intelligent microgrids. The shallow module can fast response in 0.5 s, the RMSE can reach to 62.02 W. The deep module can greatly improve the prediction accuracy, and the RMSE can reach to 20.93 W ( $R^2=0.943$ ). Even with a prediction error limit of  $\leq 3\%$ , the overall efficiency of our system can be increased by more than 30%.

The dataset is divided into 70% training set and 30% test set for validation. The traditional BP neural network and support vector machine regression (SVR) are used as reference models for contrast. The experimental results show that compared with conventional method, this model can increase the prediction accuracy by 18-22% in some complex

operation scenario. However, the computational cost of deep modules has increased by "40%", which requires a thorough trade-off between the accuracy and real-time performance of scheduling applications. The shallow module can almost be reduced to the level of a single BP network, as it only introduces the 0.26W difference between the RMSE of the training and testing sets, indicating its solid generalization ability. Error metrics are explicitly expressed in Watts (W), and detailed parameter settings are given for method reproducibility.

The prediction model can make a reliable trade-off between prediction performance and computation. Therefore, it can be used as a pragmatic tool for microgrid active power management application in real time. In the future, we will conduct additional experiment to further compare more baselines and explore the robustness of the proposed model under different climates.

## ACKNOWLEDGEMENT

The research has been funded by the The Youth Scientific and Technological Talent Cultivation Project of "Two Cities and Three Bases" of Anshun Municipal Science and Technology Bureau (No.anshunshiker-

2024-12-17-01), and the Science and Technology Research and Development Program for Higher Education Institutions, Center for Science and Technology Development, Ministry of Education (No.ZJXF2022164), and the Scientific Research Projects of Yinchuan University of Science and Technology (No. XJKY2024002).

## REFERENCES

- [1] Hassan Q., Hsu C.Y., Mounich K., Algburi S., Jaszczur M., Telba A.A., Viktor P., Awwad E.M., Ahsan M., Ali B.M., Al-Jiboory A.K., Henedy S.N., Sameen A.Z., and Barakat M., 2024. Enhancing smart grid integrated renewable distributed generation capacities: Implications for sustainable energy transformation. *Sustainable Energy Technologies and Assessments* 66: 103793. <https://doi.org/10.1016/j.seta.2024.103793>.
- [2] Dawn S., Ramakrishna A., Ramesh M., Das S.S., Rao K.D., Islam M.M., and Selim Ustun T., 2024. Integration of renewable energy in microgrids and smart grids in deregulated power systems: a comparative exploration. *Advanced Energy and Sustainability Research* 5(10): 2400088. <https://doi.org/10.1002/aesr.202400088>.
- [3] Suresh M.P., Yuvaraj T., Thanikanti S.B., and Nwulu N., 2024. Optimizing smart microgrid performance: Integrating solar generation and static VAR compensator for EV charging impact, emphasizing SCOPE index. *Energy Reports* 11: 3224-3244. <https://doi.org/10.1016/j.egy.2024.02.050>.
- [4] Kumar M.J., Sampradeepraj T., Sivajothi E., and Singh G., 2024. An efficient hybrid technique for energy management system with renewable energy system and energy storage system in smart grid. *Energy* 306: 132454. <https://doi.org/10.1016/j.energy.2024.132454>.
- [5] Arkhangelski J., Abdou-Tankari M., and Lefebvre, G., 2021. Day-ahead optimal power flow for efficient energy management of urban microgrid. *IEEE Transactions on Industry Applications*, 57(2): 1285-1293. <https://doi.org/10.1109/TIA.2020.3049117>.
- [6] Zhang B., Yan L., He Y., Huang H., Feng J., Lu L., Zhang E., Che Y., Jiang M., Liu L., and Li Z., 2021. Research on Multi-Energy Complementary Linkage Technology and Economic Evaluation. *2021 4th International Conference on Information Systems and Computer Aided Education*. 2021: 1871-1878. <https://doi.org/10.1145/3482632.3484058>.
- [7] Elgammal A. and C. Boodoo. 2021. Optimal energy management strategy for a DC linked hydro-PV-wind renewable energy system for hydroelectric power generation optimization. *European Journal of Energy Research* 1(3): 9-18. <https://doi.org/10.24018/ejenergy.2021.1.3.16>.
- [8] Kumar G.B. and K. Palanisamy. 2022. Energy management of renewable energy-based microgrid system with HESS for various operation modes. *Frontiers in Energy Research* 10: 995034. <https://doi.org/10.3389/fenrg.2022.995034>.
- [9] Barua S. and N. Mohammad. 2023. Investigating heuristic and optimization energy management algorithms to minimize residential electricity costs. *2023 International Conference on Electrical, Computer and Communication Engineering (ECCE)*. IEEE, 2023: 1-6. <https://doi.org/10.1109/ECCE57851.2023.10101630>.
- [10] Mohan H.M. and S.K. Dash. 2024. Optimized power flow management based on Harris Hawks optimization for an islanded DC microgrid. *Energy Harvesting and Systems* 11(1): 20220153. <https://doi.org/10.1515/ehs-2022-0153>.
- [11] Siddaraj S., Yaragatti U.R., and Harischandrapa N., 2023. Coordinated PSO-ANFIS-based 2 MPPT control of microgrid with solar photovoltaic and battery energy storage system. *Journal of Sensor and Actuator Networks* 12(3): 45. <https://doi.org/10.3390/jsan12030045>.
- [12] Elalfy D.A., Gouda E., Kotb M.F., and Sedhom B. E., 2023. Frequency Regulation Based on Antlion Optimization Technique for Microgrids with Electric Vehicles. *2023 24th International Middle East Power System Conference (MEPCON)*. IEEE, 2023: 1-7. <https://doi.org/10.1109/MEPCON58725.2023.10462385>.
- [13] Lv Y., Li K. Zhao, H., and Lei H., 2024. A multi-stage constraint-handling multi-objective optimization method for resilient microgrid energy management. *Applied Sciences* 14(8): 3253. <https://doi.org/10.3390/app14083253>.
- [14] Agupugo C.P., Kehinde H.M., and Manuel H.N.N., 2024. Optimization of microgrid operations using renewable energy sources. *Engineering Science and Technology Journal* 5(7): 2379-2401. <https://doi.org/10.51594/ESTJ.V5I7.1360>.
- [15] Ersöz B., Taşdelen M.C., Eren S., Sagioglu S., and Öter A., 2024. Solar energy forecasting using ensemble learning method. *2024 13th International Conference on Renewable Energy Research and Applications (ICRERA)*, IEEE, 283-287. <https://doi.org/10.1109/ICRERA62673.2024.10815583>.
- [16] Alagappan C., Ramasamy K., and Velusamy D., 2025. Bagging ensemble of artificial neural networks with weighted averaging and grey wolf optimization for solar photovoltaic power generation prediction. *International Journal of Green Energy* 22(8): 1587-1601. <https://doi.org/10.1080/15435075.2024.2436535>.
- [17] Al-Dahidi S., Ayadi O., Adeeb J., Alrbai M., and Qawasmeh B.R., 2018. Extreme learning machines for solar photovoltaic power predictions. *Energies* 11(10): 2725. <https://doi.org/10.3390/en11102725>.
- [18] Al-Dahidi S., Ayadi O., Alrbai M., and Adeeb J., 2019. Ensemble approach of optimized artificial neural networks for solar photovoltaic power prediction. *IEEE Access* 7: 81741-81758. <https://doi.org/10.1109/ACCESS.2019.2923905>.

- [19] Alrbai M., Abubaker A.M., Ahmad A.D., Al-Dahidi S., Ayadi O., Hjouj D., and Al-Ghussain L., 2022. Optimization of energy production from biogas fuel in a closed landfill using artificial neural networks: A case study of Al Ghabawi Landfill, Jordan. *Waste Management* 150: 218-226. <https://doi.org/10.1016/j.wasman.2022.07.011>
- [20] Al-Dahidi S., Muhsen H., Sari M.E.S., Alrbai M., Louzazni M., and Omran N., 2022. An adaptive approach-based ensemble for 1 day-ahead production prediction of solar PV systems. *Advances in Mechanical Engineering* 14(3): 16878132221089436. <https://doi.org/10.1177/16878132221089436>
- [21] Al-Ghussain L., Darwish Ahmad A., Abubaker A.M., Alrbai M., Ayadi O., Al-Dahidi S., and Akafuah N.K., 2023. Techno-economic assessment of photovoltaic-based charging stations for electric vehicles in developing countries. *Energy Sources, Part A: Recovery, Utilization, and Environmental Effects*, 45(1): 523-541. <https://doi.org/10.1080/15567036.2023.2171517>.
- [22] Al-Dahidi S., Adeeb J., Ayadi O., Alrbai M., and Al-Ghussain L., 2022. A feature transformation and extraction approach-based artificial neural network for an improved production prediction of grid-connected solar photovoltaic systems. *Energy Sources, Part A: Recovery, Utilization, and Environmental Effects* 44(4): 9232-9254. <https://doi.org/10.1080/15567036.2022.2128475>.

